Mindanao Journal of Science and Technology Vol. 24 (Special Issue) (2026) 71-91

Seasonal Modulation of Diurnal Precipitation over the Mentawai Islands

Aisyah Erajalita[1], Helmi Yusnaini[1], Ravidho Ramadhan[1,2], and Marzuki Marzuki[1*]

[1]Department of Physics
Universitas Andalas
Padang, 25163 Indonesia

[2]Research Institute for Sustainable Humanosphere (RISH)
Kyoto University
Gokasho, Uji, Kyoto 611-0011, Japan
[*]*marzuki@sci.unand.ac.id*

Date received: September 12, 2025
Revision accepted: August 20, 2026

Abstract

One important aspect of tropical climates is the diurnal precipitation cycle, which is strongly modulated by seasonal dynamics and atmospheric processes. This study investigates the diurnal variation of precipitation over the Mentawai Islands, a small-island region off western Sumatra that is highly exposed to heavy rainfall and hydrometeorological hazards. Hourly precipitation accumulation (PA), frequency (PF), and intensity (PI) were analyzed using IMERG V07 and GSMaP V08 satellite datasets for the wet season (November–March; NDJFM) and dry season (May–September; MJJAS) during the period 2000–2022. In addition, ERA5 reanalysis was employed to examine the associated vertical velocity, relative humidity, and surface wind convergence. The results show that PI is generally higher during the dry season (1.5–3.3 mm/h) than during the wet season (1.5–2.6 mm/h), particularly over smaller islands (Sipora and North Pagai) and adjacent coastal seas, whereas both PA and PF are greater in the wet season. Seasonal variations in vertical velocity (ω) and offshore low-level winds enhance nocturnal convection over the Mentawai Strait, leading to earlier diurnal peaks of PA and PI during MJJAS (23–01 LT) compared to NDJFM (01–03 LT) over the Mentawai Islands. In contrast, the large-scale monsoon circulation regulates the seasonal pattern of PF amplitude without significantly altering the timing of its diurnal peak. These findings not only elucidate the complex diurnal mechanisms in maritime island climates but also suggest the need for localized rainfall monitoring and early-warning systems to support ecosystem sustainability and the livelihoods of Mentawai communities that depend on nature.

Keywords*:* diurnal precipitation, seasonal, Mentawai Islands, IMERG, GSMaP

1. Introduction

The Mentawai Islands, comprising the four main islands of Siberut, Sipora, North Pagai, and South Pagai, are located off the western coast of Sumatra, Indonesia. Owing to their proximity to the equator and the Indian Ocean, these islands are highly susceptible to hydrometeorological hazards such as flooding, landslides, and coastal inundation triggered by prolonged heavy rainfall and high tides. Such events have repeatedly damaged road infrastructure, disrupted transportation networks, and adversely affected agriculture and fisheries—the primary sources of livelihood for local communities (Badan Nasional Penanggulangan Bencana [BNPB], 2023; BNPB, 2022; Ramadhan *et al.*, 2022). Over 150 flood events have been reported in recent years, closely associated with episodes of intense precipitation. Rainfall frequently reaches extreme levels in this region (Ramadhan *et al.*, 2022; Senior *et al.*, 2023), further increasing the vulnerability of local populations. The region's proximity to the Indian Ocean, where high evaporation rates favor convective cloud formation (Li *et al.*, 2016; Maheskumar *et al.*, 2014), combined with substantial moisture transport from the Indian Ocean and the western tropical Pacific (Ratna *et al.*, 2017; Yamanaka *et al.*, 2018), contributes to frequent heavy rainfall. These characteristics underscore the importance of improving early warning systems and disaster preparedness through a better understanding of precipitation behavior over the Mentawai Islands.

As a tropical island, the Mentawai Islands exhibit a prominent temporal characteristic of precipitation that is strongly influenced by the diurnal cycle of atmospheric variation (Kikuchi & Wang, 2008). This variation manifests as land–sea breeze circulations driven by solar heating, which promote convection over land (ocean) surfaces during the day (night) (M. Chen & Yao, 2023; Lapworth, 2005). Such mesoscale and synoptic-scale factors further influence the local environmental conditions over tropical islands, shaping the spatial and temporal patterns of diurnal precipitation variability (North, 2023; Wang & Sobel, 2017; Zhu *et al.*, 2017). Therefore, understanding the interaction between these factors and the diurnal cycle over the Mentawai Islands is essential for enhancing community resilience and disaster preparedness. Beyond hydrometeorological hazards, the diurnal cycle of precipitation also plays a vital role in the daily lives of local communities who remain closely connected to their natural environment. Detailed knowledge of diurnal precipitation patterns can support agricultural planning and help local fishermen avoid extreme weather conditions.

The influence of the synoptic-scale Madden–Julian Oscillation (MJO) on the diurnal cycle during the rainy season (November–March; NDJFM) over the Mentawai Islands has been examined using long-term satellite-based precipitation data (Erajalita *et al*., 2025). Their results revealed a clear secondary afternoon peak and a dominant early morning peak, particularly over the larger islands such as Siberut. This diurnal pattern during the wet season was intensified by enhanced low-level convection and convergence associated with active MJO phases, which also modified the timing of the diurnal precipitation peak. However, their analysis was limited to the wet season and did not account for the seasonal variability that shapes the diurnal cycle over the Mentawai Islands.

Seasonal variability associated with shifts in low-level winds strongly control diurnal precipitation behavior in tropical coastal regions (Aoki & Shige, 2024). For instance, Marzuki *et al*. (2024) reported that monsoon effects are more pronounced in the southern Malacca Strait and along the southern coast of Sumatra, where flat terrain limits orographic influences. The Intertropical Convergence Zone (ITCZ) exerts a greater influence on islands north of the equator than monsoon circulation, resulting in smaller seasonal variations in diurnal timing. South of the equator, however, the Bangka and Belitung Islands exhibit stronger modulation during the northwest monsoon (December to March; DJFM), producing larger diurnal amplitudes than during the dry season (May to October; MJJASO) while maintaining nearly constant peak timing throughout the seasons. These findings suggest that in low latitude island environments, the monsoonal background flow can substantially affect the amplitude of diurnal rainfall without necessarily altering its phase in eastern Sumatra.

The influence of seasonal variation on diurnal precipitation in western Sumatra has been analyzed from the perspectives of rainfall amount, frequency, intensity, and duration (Marzuki, *et al*., 2022a). It was found that short-duration rainfall events (<3 hours) dominate the southern region during December-February (DJF) and March-May (MAM) and shift northward during June-August (JJA) and September-October (SON), while long-duration events (>3 hours) exhibit a weaker seasonal shift. Despite these spatial variations, the peak timing of precipitation amount and frequency remains relatively consistent from satellite data throughout the seasons. However, rain gauge observations indicate slightly earlier rainfall peaks during JJA, likely due to enhanced solar heating and atmospheric instability. Nevertheless, rain gauge data for the Mentawai Islands were not available in that analysis. Satellite-based data were used to complement observations over coastal regions, with several cross-section points across Sumatra spaced at approximately 0.25°. Therefore, a microscale analysis of the influence of seasonal variation on the diurnal cycle in the Mentawai Islands is still required, as suggested by previous studies (Erajalita *et al.*, 2025).

2. Methodology

2.1 Study Area

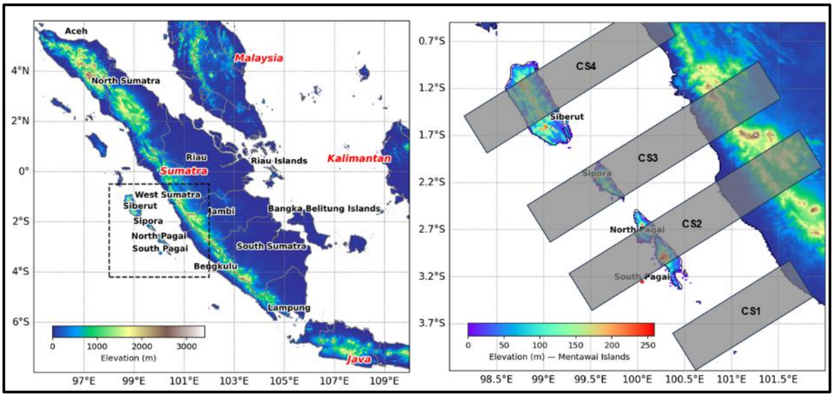

Figure 1. Topography maps of the Mentawai Islands. CS1–CS4 in panel (b) represent cross-sections used to analyze precipitation propagation from Sumatra. Elevation data used ETOPO2 from NOAA (Smith & Sandwell, 1997)

This study analyzes the seasonal modulation of diurnal precipitation over the Mentawai Islands, located off the western coast of Sumatra, Indonesia (Figure 1a). The region comprises four major islands—Siberut, Sipora, North Pagai, and South Pagai—situated near the equator and surrounded by the Indian Ocean. Several of these islands, such as South Pagai and Siberut, have relatively extensive areas with topography reaching up to 250 m above sea level. The influence of each island's topographic conditions on the propagation of rainfall from Sumatra is examined using four cross-sections (CS): CS1, which excludes the Mentawai Islands; CS2, which passes through North and South Pagai; CS3, which crosses Sipora Island; and CS4, which passes through Siberut Island (Figure 1b).

2.2 Data

The diurnal precipitation analysis in this study was conducted using high-resolution satellite-based precipitation products (SPPs). Two SPPs, namely the Integrated Multi-satellitE Retrievals for GPM (IMERG) Final Run Version 07B (Huffman *et al*., 2023) and the Global Satellite Mapping of Precipitation (GSMaP) Gauge Version 08 (Okamoto *et al*., 2004) were employed. Both datasets have the same spatial resolution of 0.1°, but differ in temporal resolution, with IMERG providing 30-minute data and GSMaP providing hourly data. The high spatial and temporal resolutions of these products make them well-suited for detailed diurnal analyses at the local scale (Ramadhan *et al*., 2023, 2024). This study utilizes long-term datasets covering the period from January 2000 to December 2022 (22 years).

In addition to precipitation data, ERA5 reanalysis data from the European Centre for Medium-Range Weather Forecasts (Hersbach *et al*., 2020) were employed to analyze the background atmospheric conditions. ERA5 provides hourly data with a horizontal resolution of 0.25°. This study focuses on vertical velocity (ω) and horizontal winds at the 925 hPa level as indicators of low-level convergence and land–sea breeze circulations that influence the diurnal cycle of precipitation.

2.3 Methods

This study was conducted in several steps. First, a data adjustment process was performed. The temporal resolution and time reference of all datasets were standardized, with IMERG data resampled to an hourly resolution and timestamps converted to Western Indonesian Time (WIB; UTC+7) as local time (LT). Subsequently, the data were classified into two seasonal periods: the wet season (November–March; NDJFM) and the dry season (May–September; MJJAS), following the peak rainfall periods over the Mentawai Islands and western Sumatra (As-syakur *et al*., 2019). April and October were excluded because they are transition months between the two monsoonal regimes, during which regional circulation and precipitation characteristics are relatively variable and may exhibit mixed seasonal signals. This seasonal classification is consistent with previous studies of rainfall and monsoonal variability over Indonesia and the tropics (Wang & Ding, 2008; Trenberth *et al.*, 2014; Marzuki *et al*., 2022a; Ramadhan *et al*., 2026). Excluding the transition months allows a clearer comparison between the two dominant monsoonal conditions.

Second, precipitation events were identified from hourly IMERG and GSMaP data. For IMERG, a precipitation event was defined as a continuous period of rainfall exceeding 0.1 mm/h, while for GSMaP, the threshold was set to 0.2 mm/h. This difference was applied because the temporal resolutions of the two datasets differ—IMERG provides data at 30-minute intervals, whereas GSMaP has a 1-hour resolution—thus, the rainfall threshold for GSMaP was set higher to maintain consistency in event detection. These thresholds are also consistent with previous studies employing the respective satellite products over Indonesia: 0.2 mm h^{-1} has been applied to GSMaP data (Satyaningsih *et al*., 2023), whereas 0.1 mm h^{-1} has been used for IMERG precipitation data (Ramadhan *et al.*, 2024; Erajalita *et al.*, 2025). A precipitation event was considered continuous if there was no interruption or if the break lasted no more than one hour. If the interruption exceeded one hour, the subsequent rainfall was regarded as a new event. The identified precipitation events were then categorized into three classes based on duration: short-duration events (< 3 hours), moderate-duration events (3–6 hours), and long-duration events (> 6 hours).

Third, diurnal precipitation parameters were derived from the identified precipitation events. These parameters include Precipitation Accumulation (PA), Precipitation Frequency (PF), and Precipitation Intensity (PI). PA was calculated as the total precipitation per hour divided by the number of observation hours. PF was computed as the percentage of time steps where rainfall exceeded 0.1 mm per interval relative to the total time steps. PI was calculated as the ratio between PA and PF. All parameters (PA, PF, and PI) were computed for each hour across a 24-hour cycle (00–23 Local Time, LT). Detailed formulations for each parameter can be found in previous studies (Marzuki *et al*., 2021; Ramadhan *et al*., 2024).

Fourth, the diurnal peak timing of PA, PF, and PI was determined through harmonic decomposition using the Fast Fourier Transform (FFT) technique. A two-order harmonic decomposition was applied to represent the diurnal (24-hour) and semidiurnal (12-hour) components. The use of harmonic decomposition is essential for identifying the true diurnal precipitation peak from satellite-based data such as IMERG and GSMaP in Indonesia (Ramadhan *et al*., 2023, 2024).

Fifth, the influence of seasonal variation on diurnal precipitation patterns over the Mentawai Islands was analyzed. After obtaining hourly PA, PF, and PI values and determining their peak timings for each IMERG and GSMaP grid, land grids were selected based on topographic data corresponding to the boundaries of the Mentawai Islands. Additionally, cross-sectional analyses were conducted by averaging PA, PF, and PI values along the defined cross-sections (Figure 1b). The diurnal precipitation characteristics for each cross-section were analyzed separately for each season to identify their differences. Furthermore, to examine the underlying physical mechanisms, ERA5 reanalysis data were used to analyze spatial variations in vertical velocity (ω) and horizontal wind components at the 925 hPa level.

3. Results and Discussion

3.1 Spatial Distribution of Average and Peak Timing of PA, PF, and PI

Figure 2 presents the spatial distributions of the average values and peak timings of PA, PF, and PI during the NDJFM and MJJAS periods, based on IMERG data. IMERG reveals that, particularly over the land areas of the Mentawai Islands, the mean PA and PF values are notably higher during NDJFM than during MJJAS. Quantitatively, the mean PA and PF during NDJFM reach approximately 0.5–0.7 mm/h and 35–55%, respectively, whereas these values decrease to about 0.35–0.6 mm/h and 20–45% during MJJAS. These magnitudes are slightly lower than those reported for mainland Sumatra by Marzuki *et al*. (2022a; 2022b), confirming that the Mentawai Islands experience lower mean precipitation intensity compared to the Sumatra mainland. Conversely, IMERG shows that the Indian Ocean and the Mentawai Strait exhibit the highest PI values during MJJAS (approximately 1.8–2.3 mm/h). It suggests stronger but more localized precipitation events during the dry season in this region. These results align with the findings of Marzuki *et al*. (2022a; 2022b), who reported substantially lower PA and PF over Sumatra during the JJA compared to other seasons.

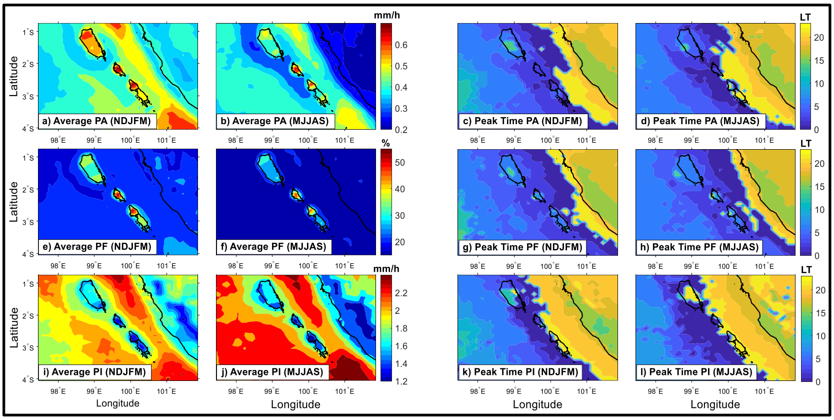

Figure 2. Mean distribution and peak times of diurnal variations of PA, PF, and PI during the rainy season (NDJFM) and summer season (MJJAS) from IMERG observations

The GSMaP dataset corroborates these observations, similarly showing higher PA (0.3–0.5 mm/h) and PF (17–25%) during NDJFM, particularly over the Mentawai Strait and the adjacent oceanic regions (Figure 3). In marked contrast, PI values increase significantly during MJJAS, reaching up to 2.8 mm/h over smaller islands such as Sipora, North Pagai, and South Pagai. This intensified PI during the dry season may be attributed to the influence of the ITCZ, which enhances local convective activity near the equatorial Indonesia even though the large-scale monsoonal moisture supply is relatively weak.

Beyond the average PA, PF, and PI values, both IMERG and GSMaP consistently show pronounced diurnal rainfall peaks (Figures 2, 3). Rainfall peak timing predominantly occurs from early morning to dawn over the Mentawai Islands and from midnight to nighttime over adjacent oceans in both the NDJFM and MJJAS seasons. Nevertheless, the timing of peak PA, PF, and PI reveals a non-uniform pattern across both the straits between the Mentawai Islands and Sumatra, and the land areas of the Mentawai Islands, across the two seasons. This seasonal variation of peak timing of diurnal cycle indicates significant seasonal variation within the Mentawai Islands region.

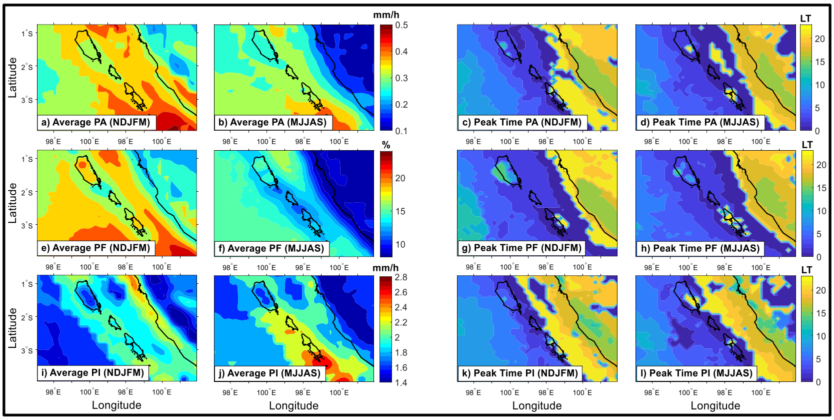

Figure 3. Mean distribution and peak times of diurnal variations of PA, PF, and PI during the rainy season (NDJFM) and summer season (MJJAS) from GSMaP observations

3.2 Diurnal PA, PF, and PI over Mentawai Mainland

To provide a clearer depiction of the diurnal variability between NDJFM and MJJAS over the Mentawai mainland, the hourly time series of PA, PF, and PI are presented in Figure 4. Distinct differences between the two satellite precipitation products (SPPs) are evident, where GSMaP consistently exhibits lower PA values compared to IMERG across all islands. The lower PA values in GSMaP are accompanied by substantially underestimated PF values, particularly over Sipora and North Pagai (Figure 4f, g). This discrepancy arises mainly from the differing temporal resolutions of the two datasets, which lead to variations in rainfall event detection depending on the applied threshold.

In addition to the overall underestimation, PF values derived from both datasets display different diurnal peak times and patterns across the islands. Conversely, GSMaP shows higher PI values than IMERG, especially over the smaller islands (Figure 4j–l). These findings highlight the need for further quantification of the accuracy of both SPPs in capturing the diurnal cycle over small islands, particularly through comparison with ground-based observations in the Mentawai Islands.

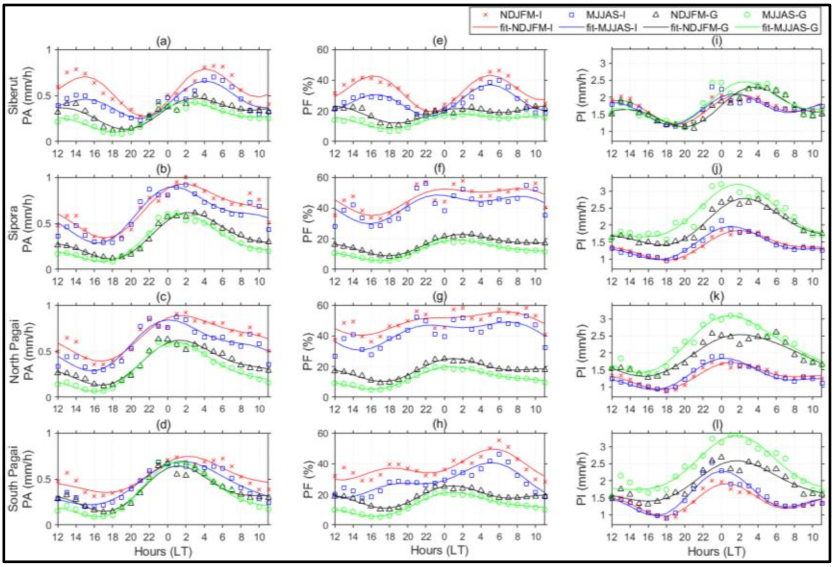

Figure 4. Average diurnal variations of PA (a–d), PF (e–h), and PI (i–l) for the four Mentawai Islands during NDJFM and MJJAS, derived from IMERG and GSMaP observations. The legend uses G and I to denote GSMaP and IMERG datasets, respectively. The lines labeled fit represent a second-order harmonic fitting applied to the direct PA, PF, and PI calculations for each dataset

Although PF values from IMERG and GSMaP are not consistent, both datasets exhibit similar diurnal patterns in PA and PI. The PA pattern on each island is more strongly influenced by PI than by PF, indicating that high-intensity rainfall events dominate the total rainfall volume over the Mentawai Islands. Except for Siberut, all islands show a single early-morning (00–04 LT) peak in both PA and PI. In contrast, Siberut exhibits two PA peaks, with the early-morning peak occurring slightly later (04–06 LT) and an additional afternoon peak around 14–16 LT. The dominance of early-morning heavy rainfall over the Mentawai Islands is attributed to the propagation of convective systems from Sumatra (Erajalita *et al*., 2025).

Seasonal variations in the magnitudes of PF and PI are clearly observed across the Mentawai Islands (Figure 4). PF values are consistently higher during NDJFM than during MJJAS, whereas PI values are generally higher during MJJAS. These seasonal differences in PF and PI are more evident over Sipora, North Pagai, and South Pagai. For these islands, PF values during NDJFM (MJJAS) range from 49–56% (40–49%) and 22–26% (19–21%) for IMERG and GSMaP, respectively. Meanwhile, the corresponding PI magnitudes are 1.7 – 1.9 mm h^{-1} (1.8–2.3 mm h^{-1}) and 2.5–2.8 mm h^{-1} (3–3.3 mm h^{-1}) from IMERG and GSMaP during NDJFM (MJJAS). In contrast, over Siberut, the differences in PF are larger than those in PI, with PF and PI magnitudes during NDJFM (MJJAS) of 43%(37%) and 2.08 mm h^{-1} (2.1 mm h^{-1}) from IMERG, and 22%(18%) and 2.3 mm h^{-1} (2.5 mm h^{-1}) from GSMaP. These results indicate that although nocturnal rainfall occurs more frequently during NDJFM, rainfall intensity tends to be stronger during MJJAS.

In addition to magnitude differences, variations in the diurnal peak timing between seasons are also observed across the Mentawai Islands (Figure 4). Peak-time differences are more distinct in IMERG than in GSMaP, reflecting the higher reliability of half-hourly data compared to hourly data for precise diurnal analysis. Overall, the early-morning peaks of PA, PF, and PI during MJJAS occur one to two hours earlier than those during NDJFM. This suggests that seasonal differences influence the speed of offshore rainfall propagation from Sumatra toward the Indian Ocean.

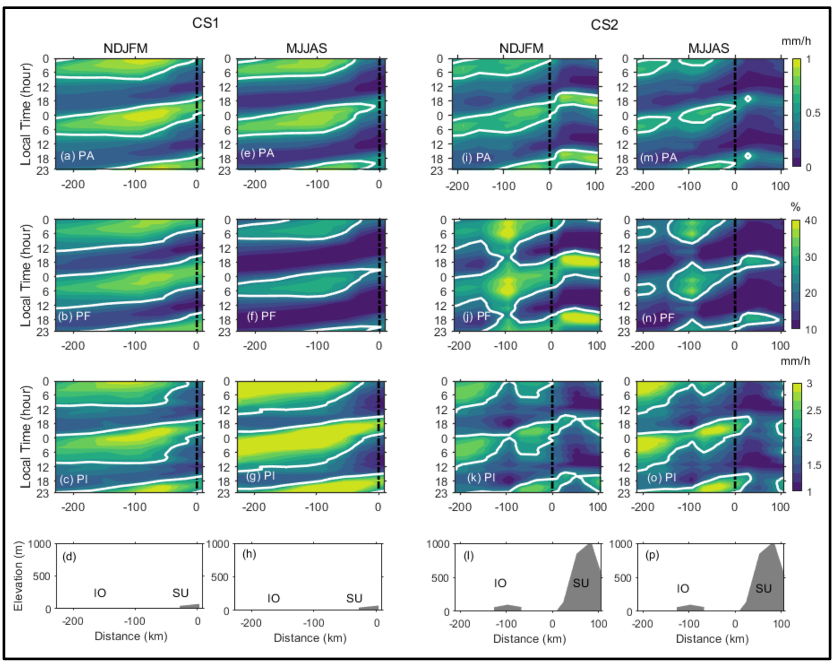

Figure 5. Local time–distance cross-sections of PA, PF, and PI along the CS1 and CS2 zones of the Mentawai Islands region. Vertical broken lines at 0 km indicate the locations of the Sumatran coastlines. Sumatra and the Indian Ocean are

denoted by SU and IO, respectively, in panels d, h, l, and p. Westward movement is directed to the left.

3.3 Seasonal Variation of Diurnal Propagation of Precipitation

Figures 5 and 6 present the local time–distance cross-sections of PA, PF, and PI along all cross-sections indicated in Figure 1b, based on IMERG data. IMERG was selected for this diurnal rainfall propagation analysis due to its higher temporal resolution, which allows for a better representation of seasonal variability compared to GSMaP (Figure 4). The white contour lines indicate PA, PF, and PI values exceeding 0.5 mm/h, 25%, and 2 mm/h, respectively.

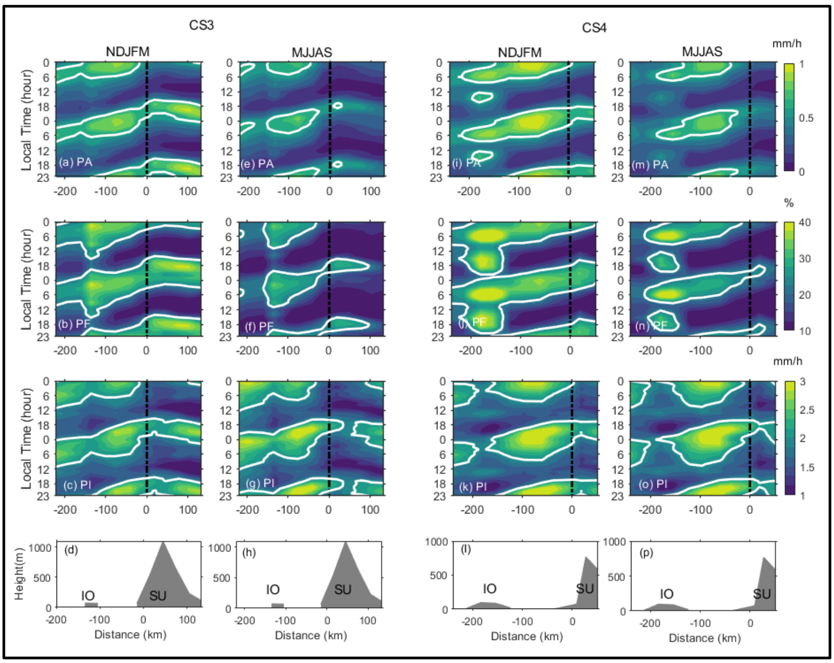

Figure 6. Local time–distance cross-sections of PA, PF, and PI along the CS3 and CS4 zones of the Mentawai Islands region. Vertical broken lines at 0 km indicate the locations of the Sumatran coastlines. Sumatra and the Indian Ocean are denoted by SU and IO, respectively, in panels d, h, l, and p. Westward movement is directed to the left.

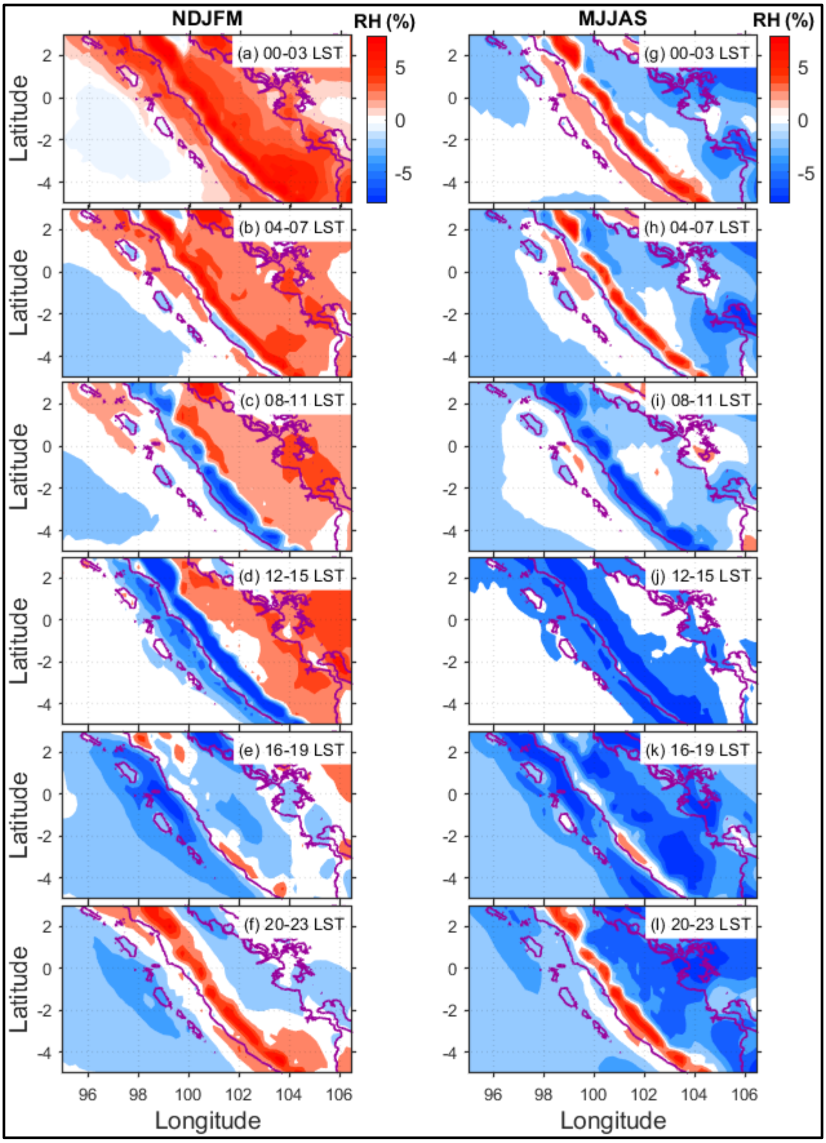

Figure 7. Distribution of RH anomalies every 4 hours from 00 to 23 LT (top to bottom), obtained from ERA5 data and averaged over NDJFM (left, a-f) and MJJAS (right, g-l) for 2000 to 2022

Over the oceanic region without islands (CS1), clear offshore propagation of rainfall from Sumatra can be observed in both PA and PF during NDJFM, while PI shows a more pronounced signal during MJJAS (Figure 5c,g). In addition to CS1, higher PI values are also detected over the Mentawai Strait during MJJAS compared to NDJFM (Figures 5 and 6). Moreover, PI during MJJAS tends to persist longer than during NDJFM. This condition can be explained by the contrasting characteristics of vertical velocity (ω) and relative humidity (RH) between the two seasons (Figures 7 and 8). Negative ω, which indicates upward air motion, is more prevalent during 00–03 LT in MJJAS over the Mentawai Strait compared to NDJFM, consistent with the higher PI values during that season. Conversely, RH anomalies are generally higher during NDJFM, suggesting a more abundant water vapor source that supports more persistent rainfall. Thus, although local factors contribute to convection-related processes, large-scale meteorological patterns largely control the precipitation characteristics over the Mentawai Islands (Bae & Min, 2022; Inoue *et al*., 2020).

In addition to amplitude differences, PA and PI propagation across all cross-sections show slightly higher propagation speeds during MJJAS compared to NDJFM (Figures 5 and 6). This faster propagation during MJJAS is associated with prevailing offshore low-level background winds, as opposed to onshore winds during NDJFM (Figure 8). These findings are consistent with Aoki and Shige (2024), who reported that offshore propagation tends to start earlier and move faster under moderate to strong offshore low-level winds.

However, there is no general consensus regarding the role of low-level winds in controlling the speed of offshore rainfall propagation (Z. Chen *et al*., 2025; Peatman *et al*., 2023; Zhou *et al*., 2022). One proposed explanation is that diurnal precipitation propagation under different wind regimes is driven by coastal gravity waves triggered by land–sea thermal contrasts (Aoki & Shige, 2024). Stronger background winds can induce Doppler shifts and advect coastal gravity waves, leading to asymmetric diurnal precipitation patterns with differing propagation speeds between upwind and downwind sides. Although the diurnal cycle of coastal precipitation can be well explained by gravity-wave dynamics in a climatological context (long-term averages), the contribution of such waves to individual precipitation events remains uncertain. Therefore, further analyses of individual rainfall events using more comprehensive observational data are needed to better understand these processes.

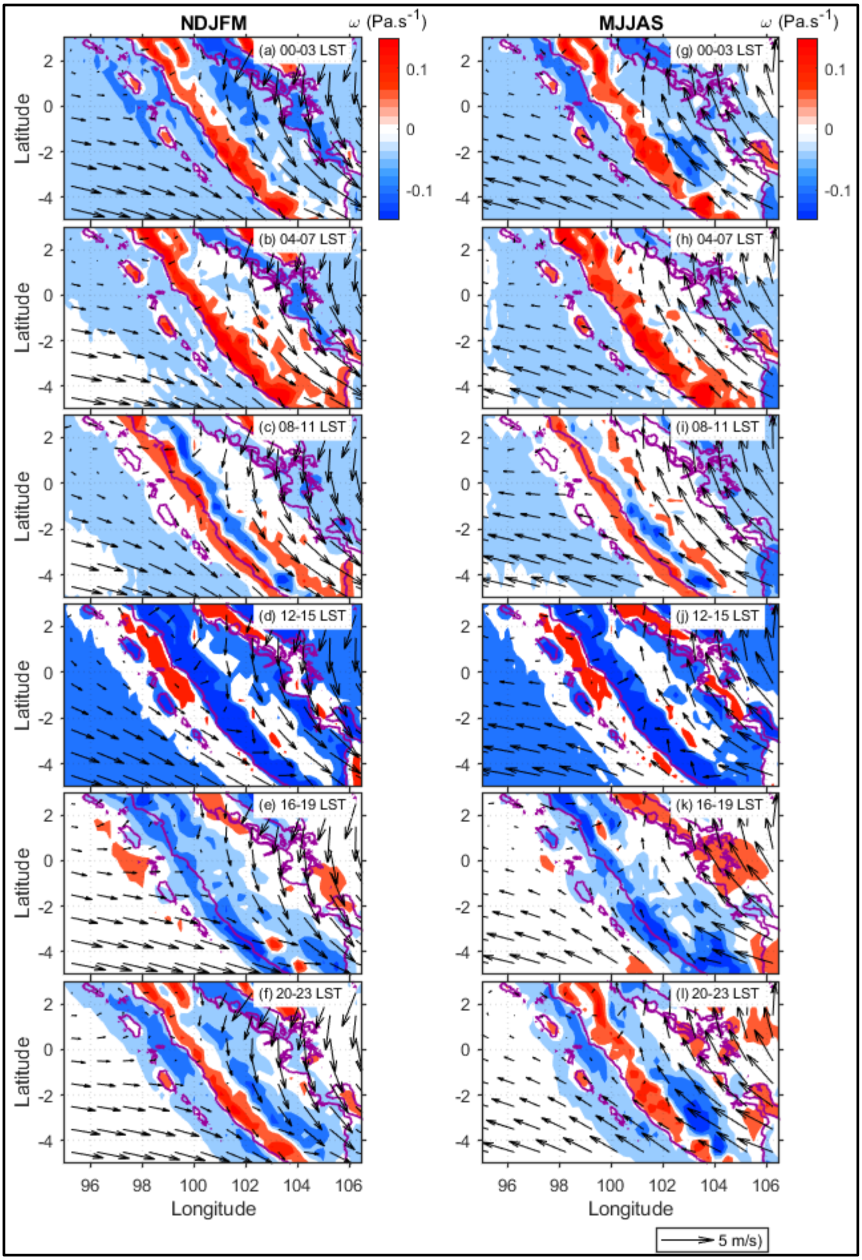

Figure 8. Distribution of ω and 925 hPa horizontal wind anomalies every 4 hours from 00 to 23 LT (top to bottom), obtained from ERA5 data and averaged over NDJFM (left, a–f) and MJJAS (right, g–l) for 2000–2022

The observed seasonal variability of offshore precipitation propagation from western Sumatra toward the Indian Ocean through the Mentawai Islands underscores the importance of validating weather and climate models in estimating diurnal peak timing (Love *et al.*, 2011). Although current model predictions still struggle with individual events, the IMERG results indicate that peak rainfall intensity occurs earlier during MJJAS than during NDJFM over the Mentawai Islands. This information could be utilized to improve early warning systems. During NDJFM, preparedness should emphasize widespread and prolonged rainfall, whereas during MJJAS, attention should focus on short-duration but high-intensity events that may trigger flash floods or coastal runoff. Implementing automated rain-gauge networks and integrating satellite-based nowcasting could enhance disaster risk reduction and agricultural planning in the insular environment of the Mentawai Islands.

4. Conclusions and Recommendation

The diurnal precipitation cycle over the Mentawai Islands exhibits opposite variations in amplitude and peak timing of precipitation frequency and intensity between November–March (NDJFM) and May–September (MJJAS). The amplitudes of PA and PF reach their maximum during NDJFM, whereas PI shows a higher amplitude during MJJAS. ERA5 relative humidity (RH) data indicate that the elevated PF during NDJFM is associated with an abundant water vapor source during this period. In contrast, vertical velocity (ω) and low-level wind patterns reveal stronger offshore winds and enhanced updrafts during MJJAS over the Mentawai Islands. In addition to higher PI values, the offshore propagation of rainfall from Sumatra occurs more rapidly during MJJAS, resulting in an earlier nocturnal rainfall peak over the Mentawai Islands—approximately two hours earlier than during NDJFM. Practically, these findings support the development of localized rainfall monitoring and early-warning systems, as well as adaptive water resource management strategies aimed at enhancing the resilience of Mentawai communities to hydrometeorological hazards.

This study is limited to a two-season classification. Although these two periods are characterized by distinct large-scale circulation patterns, the influence of low-level background wind variability within each season should be further considered. Future studies are encouraged to classify days based on low-level wind and ω conditions in the Mentawai Strait within each season.

Analyzing diurnal rainfall patterns under such classifications would improve understanding of the offshore propagation mechanisms in this region. Furthermore, combining ground-based observations with satellite datasets is strongly recommended for day-to-day event analysis under the proposed classification scheme.

5. Acknowledgement

This research was funded by the 2024 Postgraduate Research Master's Thesis of the Ministry of Education, Culture, Research and Technology/Directorate General of Higher Education, Research and Technology (Contract No: 041/E5/PG.02.00.PL/2024 and 160/UN16.19/PT.01.03/PL/2024). We also express our gratitude to NASA and JAXA for providing the IMERG and GSMaP satellite precipitation data, and to the European Centre for Medium-Range Weather Forecasts (ECMWF) for making the ERA5 reanalysis data available.

6. References

Aoki, S., & Shige, S. (2024). Control of low-level wind on the diurnal cycle of tropical coastal precipitation. *Journal of Climate, 37*(1), 229–247. https://doi.org/10.1175/JCLI-D-23-0180.1

As-syakur, A.R., Imaoka, K., Ogawara, K., Yamanaka, M.D., Tanaka, T., Kashino, Y., Nuarsa, I.W., & Osawa, T. (2019). Analysis of spatial and seasonal differences in the diurnal rainfall cycle over Sumatera revealed by 17-Year TRMM 3B42 dataset. *Sola, 15*, 216–221. https://doi.org/10.2151/sola.2019-039

Bae, J.-H., & Min, K.-H. (2022). Forecast characteristics of radar data assimilation based on the scales of precipitation systems. *Remote Sensing, 14*(3), 605. https://doi.org/10.3390/rs14030605

Badan Nasional Penanggulangan Bencana [BNPB]. (2022). Annual Performance Report of the National Disaster Management Agency for FY 2022. https://bnpb.go.id/laporan-kinerja-tahunan-badan-nasional-penanggulangan-bencana-ta-2022

Badan Nasional Penanggulangan Bencana [BNPB]. (2023). Laporan Harian PUSDALOPS BNPB. https://pusdalops.bnpb.go.id/2023/08/28/laporan-harian-pusdalops-bnpb-jumat-24-agustus-2023/

Chen, M., & Yao, X. (2022). The characteristics and mechanisms on diurnal variation of summer precipitation over the Tibetan Plateau. *Climate Dynamics, 60*(7–8), 2405–2418. https://doi.org/10.1007/s00382-022-06423-w

Chen, Z., Du, Y., Vincent, C., Short, E., & Yang, H. (2025). Influence of coastal topography on offshore diurnal rainfall propagation dynamics: a linear gravity wave model approach. *Journal of the Atmospheric Sciences, 82*(9), 1911–1927. https://doi.org/10.1175/JAS-D-24-0214.1

Erajalita, A., Marzuki, M., Yusnaini, H., Ramadhan, R., & Vonnisa, M. (2025). Influence of madden-julian oscillation on diurnal precipitation dynamics in the Mentawai Islands: a high-resolution satellite perspective. *Atmospheric Research, 325*, 108234. https://doi.org/10.1016/j.atmosres.2025.108234

Hersbach, H., Bell, B., Berrisford, P., Hirahara, S., Horányi, A., Muñoz-Sabater, J., Nicolas, J., Peubey, ... & Thépaut, J. (2020). The ERA5 global reanalysis. *Quarterly Journal of the Royal Meteorological Society, 146*(730), 1999–2049. https://doi.org/10.1002/qj.3803

Huffman, G.J., Bolvin, D.T., Joyce, R., Kelley, O.A., Nelkin, E.J., Portier, A., Stocker, E.F., Tan, J., Watters, D.C., & West, B.J. (2023). IMERG V07 Release Notes.

Inoue, K., Adames, Á. F., & Yasunaga, K. (2020). Vertical velocity profiles in convectively coupled equatorial waves and MJO: new diagnoses of vertical velocity profiles in the wavenumber–frequency domain. *Journal of the Atmospheric Sciences, 77*(6), 2139–2162. https://doi.org/10.1175/jas-d-19-0209.1

Kikuchi, K., & Wang, B. (2008). Diurnal precipitation regimes in the global tropics. *Journal of Climate, 21*(11). https://doi.org/10.1175/2007JCLI2051.1

Lapworth, A. (2005). The diurnal variation of the marine surface wind in an offshore flow. *Quarterly Journal of the Royal Meteorological Society, 131*(610), 2367–2387. https://doi.org/10.1256/qj.04.161

Li, Z., Lau, W. K.-M., Ramanathan, V., Wu, G., Ding, Y., Manoj, M. G., Liu, J., Qian, Y., … & Brasseur, G. P. (2016). Aerosol and monsoon climate interactions over Asia. *Reviews of Geophysics, 54*(4), 866–929. https://doi.org/10.1002/2015RG000500

Love, B.S., Matthews, A.J., & Lister, G.M.S. (2011). The diurnal cycle of precipitation over the maritime continent in a high-resolution atmospheric model. *Quarterly Journal* *of the Royal Meteorological Society, 137*(657), 934 – 947. https://doi.org/10.1002/qj.809

Maheskumar, R.S., Narkhedkar, S.G., Morwal, S.B., Padmakumari, B., Kothawale, D.R., Joshi, R.R., Deshpande, C.G., Bhalwankar, R.V., & Kulkarni, J.R. (2014). Mechanism of high rainfall over the Indian West Coast Region during the monsoon season. *Climate Dynamics, 43*(5–6), 1513–1529. https://doi.org/10.1007/s00382-013-1972-9

Marzuki, M., Suryanti, K., Yusnaini, H., Tangang, F., Muharsyah, R., Vonnisa, M., & Devianto, D. (2021). Diurnal variation of precipitation from the perspectives of precipitation amount, intensity and duration over Sumatra from rain gauge observations. *International Journal of Climatology, 41*(8), 4386–4397. https://doi.org/10.1002/joc.7078

Marzuki, M., Yusnaini, H., Tangang, F., Muharsyah, R., Vonnisa, M., & Harmadi, H. (2022a). Land – sea contrast of diurnal cycle characteristics and rain event propagations over Sumatra according to different rain duration and seasons. *Atmospheric Research, 270*, 106051. https://doi.org/10.1016/j.atmosres.2022.106051

Marzuki, M., Yusnaini, H., Ramadhan, R., Tangang, F., Amirudin, A.A. Bin, Hashiguchi, H., Shimomai, T., & Vonnisa, M. (2022b). Characteristics of precipitation diurnal cycle over a mountainous area of Sumatra Island including MJO and seasonal signatures based on the 15-year optical rain gauge Data, WRF Model and IMERG. *Atmosphere, 13*(1), 63. https://doi.org/10.3390/atmos13010063

Marzuki, M., Yusnaini, H., Ramadhan, R., Muharsyah, R., Vonnisa, M., Harmadi, H., & Tangang, F. (2024). Diurnal cycle of precipitation over coastal sea and small islands in the Eastern Region of Sumatra including season and madden julian oscillation signatures. *Atmospheric Research, 299*, 107180. https://doi.org/10.1016/j.atmosres.2023.107180

North, R.T. (2023). Land and sea breeze characteristics off the West Coast of Sumatra (Thesis). Texas A&M University, College Station, Texas, United States

Okamoto, K., Iguchi, T., Hanado, H., Takahashi, N., & Ushio, T. (2004). The Global Satellite Mapping of Precipitation (GSMaP) Project: Part I Outline of the Project. The 2nd TRMM International Science Conference, Nara.

Peatman, S.C., Birch, C.E., Schwendike, J., Marsham, J.H., Dearden, C., Webster, S., Neely, R.R., & Matthews, A.J. (2023). The role of density currents and gravity waves in the offshore propagation of convection over Sumatra. *Monthly Weather Review, 151*(7), 1757–1777. https://doi.org/10.1175/MWR-D-22-0322.1

Ramadhan, R., Marzuki, M., Yusnaini, H., Muharsyah, R., Suryanto, W., Sholihun, S., Vonnisa, M., Battaglia, A., & Hashiguchi, H. (2022). Capability of GPM IMERG products for extreme precipitation analysis over the Indonesian maritime continent. *Remote Sensing, 14*(2), 412. https://doi.org/10.3390/rs14020412

Ramadhan, R., Marzuki, M., Yusnaini, H., Muharsyah, R., Tangang, F., Vonnisa, M., & Harmadi, H. (2023). A preliminary assessment of the GSMaP version 08 products over Indonesian maritime continent against gauge data. *Remote Sensing, 15*(4), 1115. https://doi.org/10.3390/rs15041115

Ramadhan, R., Marzuki, M., Suryanto, W., Sholihun, S., Yusnaini, H., & Muharsyah, R. (2024). Validating IMERG data for diurnal rainfall analysis across the Indonesian maritime continent using gauge observations. *Remote Sensing Applications: Society and Environment, 34,* 101186. https://doi.org/10.1016/j.rsase.2024.101186

Ramadhan, R., Hanif, M., Marzuki, M., Hashiguchi, H., Harjupa, W., & Yusnaini, H. (2026). Spatio-temporal variability of hydrometeorological disasters in Indonesia based on national disaster risk management data. *International Journal of Disaster Risk Reduction*, 143, 106256. https://doi.org/10.1016/j.ijdrr.2026.106256

Ratna, S., Ratnam, J., Behera, S., Tangang, F., & Yamagata, T. (2017). Validation of the WRF regional climate model over the subregions of Southeast Asia: climatology and interannual variability. *Climate Research, 71*(3), 263–280. https://doi.org/10.3354/cr01445

Satyaningsih, R., Jetten, V., Ettema, J., Sopaheluwakan, A., Lombardo, L., & Nuryanto, D. E. (2023). Dynamic rainfall thresholds for landslide early warning in Progo Catchment, Java, Indonesia. *Natural Hazards*, 119(3), 2133-2158. https://doi.org/10.1007/s11069-023-06208-2

Senior, N.V., Matthews, A.J., Webber, B.G.M., Webster, S., Jones, R.W., Permana, D. S., Paski, J.A.I., & Fadila, R. (2023). Extreme precipitation at Padang, Sumatra triggered by convectively coupled kelvin waves. *Quarterly Journal of the Royal Meteorological Society, 149*(755), 2281–2300. https://doi.org/10.1002/qj.4506

Smith, W.H.F., & Sandwell. D.T. (1997). Global sea floor topography from satellite altimetry and ship depth soundings. *Science, 277,* 1956-1962. https://doi.org/10.1126/science.277.5334.1956

Trenberth, K. E., Fasullo, J. T., Branstator, G., & Phillips, A. S. (2014). Seasonal aspects of the recent pause in surface warming. *Nature Climate Change,* 4(10), 911-916. https://doi.org/10.1038/nclimate2341

Wang, S., & Sobel, A. H. (2017). Factors controlling rain on small tropical islands: diurnal cycle, large-scale wind speed, and topography. *Journal of the Atmospheric Sciences*, *74*(11), 3515–3532. https://doi.org/10.1175/JAS-D-16-0344.1

Wang, B., & Ding, Q. (2008). Global monsoon: Dominant mode of annual variation in the tropics. *Dynamics of Atmospheres and Oceans*, 44(3-4), 165-183. https://doi.org/10.1016/j.dynatmoce.2007.05.002

Yamanaka, M. D., Ogino, S.-Y., Wu, P.-M., Jun-Ichi, H., Mori, S., Matsumoto, J., & Syamsudin, F. (2018). Maritime continent coastlines controlling earth's climate. *Progress in Earth and Planetary Science, 5*(1), 21. https://doi.org/10.1186/s40645-018-0174-9

Zhou, Y., Wang, S., & Fang, J. (2022). Diurnal cycle and dipolar pattern of precipitation over Borneo during an MJO Event: lee convergence and offshore propagation. *Journal of the Atmospheric Sciences, 79*(8), 2145–2168. https://doi.org/10.1175/JAS-D-21-0258.1

Zhu, L., Meng, Z., Zhang, F., & Markowski, P.M. (2017). The influence of sea- and land-breeze circulations on the diurnal variability of precipitation over a tropical island. *Atmospheric Chemistry and Physics, 17*(21), 13213–13232. https://doi.org/10.5194/acp-2017-332